Medical University
"Prof. Dr. Paraskev Stoyanov" – Varna
Faculty of Pharmacy
Department of Physics and Biophysics

Natalina Konstantinova Panova

Corrosion resistance of AISI 321 austenitic steel in biological fluids after laser surface treatment

ABSTRACT

of dissertation
for the acquisition
of PhD educational and scientific degree

SCIENTIFIC FIELD

Medical Physics

SCIENTIFIC SUPERVISORS:

1. Prof. Tsanka Dikova, DSc, PhD, Mech Eng
2. Prof. Krastena Nikolova, PhD

Varna, 2024

The dissertation has been approved and referred for defense at a meeting of the Department of Physics and Biophysics at the Faculty of Pharmacy, Medical University "Prof. Dr. Paraskev Stoyanov" – Varna.

The dissertation contains 127 standard pages and is illustrated with 9 tables and 65 figures. The Reference consists of 180 sources, 3 of which are in Cyrillic and 177 in Latin.

The public defense of the dissertation will take place on May 31, 2024 at 11:00 a.m. in Hall School for PhD students, MU – Varna, and online through the Webex platform before a scientific jury of the following members:

Chair:

Prof. Lubomir Makedonski, PhD – external member

Members:

Prof. Jordan Maximov, DSc, PhD, Mech Eng – external member
Prof. Plamen Zagorchev, DSc, PhD – external member
Prof. Mariya Marudova-Zsivanovits, PhD – external member
Prof. Daniela Kovacheva, PhD – external member

The defense materials are available at the Scientific Department of MU – Varna and are published on the website of MU – Varna.

Note: The numbers of formulas, tables and figures in the abstract correspond to the numbers in the dissertation.

CONTENT

NOTATIONS

λ – laser wavelength, nm
η – coefficient of useful action, taking into account the efficiency of using the source energy
τ – interraction time, s
E – laser beam energy, J
S – area of the interraction spot, cm^2
d – diameter of the impact spot, cm
v – speed of movement of the source on the surface, cm/s
N – effective power of the beam, W
Nl – laser output power, W
Ns – impact power density, W/cm^2
Es – impact energy density, J/cm^2
Ev – specific volumetric energy, J/cm^3
Ef – free potential, mV
Ess – free potential stationary value, mV
Ecor – average corrosion potential, mV
icorr – corrosion current, mA
Epit – pitting potential, mV

ABBREVIATIONS

SLA – Stereolithography
SLM – Selective laser melting
FDM – Fused deposition modeling
IJP – Ink-jet printing
CAD/CAM – Computer Aided Design/Computer Aided Manufacturing
EDX – Energy-dispersive X-ray spectroscopy
SCE – Standard Reference Electrode – Saturated Calomel Electrode
HBE – Normal Hydrogen Electrode
PBS – Phosphate buffered saline
SBF – Simulated body fluids
AISI 304 – Austenitic chrome-nickel stainless steel
AISI 304L – Austenitic low-carbon chrome-nickel stainless steel (L for Low)
AISI 321 (EN X6CrNiTi 18-10, X18H10T GOST) – Austenitic chrome-nickel stainless steel
AISI 316L – Austenitic low-carbon chrome-nickel stainless steel (L for Low)
HV – Vickers hardness
KTP – Solid-state laser using potassium titanyl phosphate crystal
SLS – Selective laser sintering
PMMA – Polymethyl methacrylate
OM – Optical microscope
SEM – Scanning electron microscope
PDCs – Potentiodynamic curves
AS – Artificial saliva
MZ – Molten zone
TIZ – Thermal influence zone

INTRODUCTION

Austenitic stainless steels have been one of the first alloys used to fabricate implants, structures and devices for the general and dental medicine, due to their high corrosion resistance and good mechanical properties. Their composition includes low carbon content (< 0.03%), high chromium (15–20%) and nickel (3-14%) content, manganese (1-7.5%) and minimum amounts of other alloying elements (Si, Mo, Nb, Ti). The presence of nickel and manganese stabilizes the austenite structure at room temperature. The corrosion resistance of these steels is due, on the one hand, to the single-phase austenite structure, and on the other hand, to chromium passivating effect. Due to the presence of a large amount of chromium, a dense thin layer of Cr_2O_3 is formed on the steel surface, which protects the structure from further penetration of oxygen and other elements from the corrosive medium into the metal. Of the austenitic stainless steels, AISI 316 L, is the most widely used in medicine to fabricate coronary stents, orthopedic implants and fracture fixation devices. Other austenitic stainless steels that find biomedical applications are AISI 304, AISI 304L, and AISI 321. These are mainly used for the production of orthodontic wires and bands for dentistry.

In recent years, laser technologies have been widely implemented in the production of various types of implants and medical devices. Laser cutting is used for the fabrication of stents, selective laser melting and laser welding – for the production of customized implants and structures with a complex shape, laser heat treatment – to improve the properties on the surface of the parts. The implementation of these technologies, however, leads to changes in the microstructure of the treated surface layer, which can lead to changes in the corrosion resistance and mechanical properties.

Implants, dental structures and medical devices are used under conditions of aggressive biological fluids at the temperature of the human body. Body fluids are highly corrosive because they contain chloride, hydroxide and other ions, bacteria, proteins and dissolved oxygen. The human body is characterized by pH 7.4; however, after

surgeries or due to hematomas, inflammations or infections, this value may vary between 4 and 9. Such changes increase the risk of corrosion and the release of metal ions that can cause certain cytotoxic effects. Therefore, it is important that the materials and technologies used to make implants and dental structures ensure high properties and corrosion resistance. On the other hand, the rapid development of materials and production technologies in the recent years leave the issue of investigating the properties and especially the corrosion resistance constantly relevant.

CHAPTER 1
CORROSION RESISTANCE IN BIOLOGICAL FLUIDS OF AUSTENITE STAINLESS STEELS AFTER SURFACE IMPACT WITH LASER

A literature review of the application of lasers and laser technologies in modern dentistry, stainless steels for biomedical applications and the corrosion of stainless steels, has been made. It has been established that under the conditions of introducing laser technologies in the fabrication of customized implants from bio-compatible metals and alloys, it is necessary to carry out studies of the microstructure in the zones of laser impact and its influence on the performance properties, in particular the corrosion resistance in biological fluids.

OBJECTIVE OF THIS DISSERTATION:

To study AISI 321 austenitic stainless steel corrosion resistance in biological fluids after laser surface treatment.

TASKS:

1. To investigate the AISI 321 austenitic steel surface microstructure after laser melting and make a comparative analysis with the untreated material microstructure.

2. To investigate the corrosion resistance of AISI 321 steel laser-molten layers in Ringer's saline.
   a) To carry out experiments using specimen immersion;
   b) To investigate the electrochemical corrosion in Ringer's saline.
3. To investigate the corrosion destruction of AISI 321 steel laser-molten layers in Ringer's saline.
4. To investigate the electrochemical corrosion of AISI 321 steel laser-molten layers in artificial saliva.
   a) To investigate steel corrosion behavior in high acidity artificial saliva;
   b) To make a comparative analysis of the electrochemical corrosion in artificial saliva of various acidity.

CHAPTER 2
MATERIALS AND METHODS

2. Material and methods of specimen making.

2.1. Specimen material and dimensions

In the recent years, austenitic stainless steel AISI 316L, which is a low-carbon (L for Low) chrome-nickel steel, has been mainly used in general and dental medicine. Other austenitic stainless steels that find biomedical application are AISI 304, AISI 321, and AISI 304L [Dikova, Ts., 2014].

As studies are mainly conducted with AISI 316 steel, AISI 321 steel (EN X6CrNiTi 18-10, X18H10T GOST) with the chemical composition presented in Table 2-1 was used in this study:

Table 2-1

Chemical composition of X18H10T steel specimens (weight %).

Chemical element → / Steel ↓	C, %	Cr, %	Ni, %	Si, %	Mn, %	P, %	S, %	Ti, %	Fe, %
AISI 321	0.075	18.20	10.85	0.98	1.82	0.042	0.012	0.52	Res.

The initial specimens were prismatic with dimensions 10 mm x 30 mm x 100 mm and were made by milling.

2.2. Laser surface treatment of specimens

One surface of each specimen was treated using continuous CO_2 laser with initial power $N_Л$ = 1.2 kW and wavelength λ = 10.6 μm. Laser processing was implemented via modes guaranteeing various melting depths of the surface layer (Table 2-2). Technological parameters were determined by formulas (6) and (7). Surface treatment created a laser-molten layer 0.2-0.5 mm deep and 4 mm wide. To reduce the significant roughness of the surface after laser melting, the specimens were ground carefully and one of them (number 6) was polished.

Table 2-2

Technological parameters of laser surface treatment.

Specimen	d cm	v cm/s	N_s W/cm^2	E_v J/cm^3	Surface condition
0	-	-	-	-	Ground
1	0.4	0.3	9.5	31.7x10^3	Ground
4	0.3	0.5	17	34.4x10^3	Ground
6	0.3	0.6	17	28.3x10^3	Ground and polished

3. Corrosion study

AISI 321 steel corrosion was studied using two methods: by immersing the specimens in the corrosion medium and by electrochemical corrosion. Two corrosion media, Ringer's saline and artificial saliva, were used with the chemical composition shown in Table 2-3. The artificial saliva (Fusayama, Meyer) was prepared in the chemical laboratory of the Faculty of Pharmacy – Varna.

Table 2-3
Chemical composition of Ringer's saline and artificial saliva used in the corrosion study.

Composition	Ringer's saline g/L	Artificial saliva (Fusayama, Meyer) g/L	Artificial saliva with high acid levels g/L
NaCl	9.00	0.40	0.40
KCl	0.42	0.40	0.40
$CaCl_2$	0.48	-	-
$CaCl_2 \cdot 2H_2O$	-	0.906	0.906
$NaHCO_3$	0.20	-	-
$NaH_2PO_4 \cdot 2H_2O$	-	0.690	0.690
$Na_2S.9H_2O$	-	0.005	0.005
Urea	-	1.000	1.000
Acetic acid	-	-	+
pH (~)	6.4	6.5	5.6

Since saliva acid levels in the oral cavity vary between 5.2-7.8 pH, the electrochemical corrosion was investigated in two pH variants: 6.5 and 5.6. Acetic acid was used to lower the pH level.

3.1. Corrosion tests by specimen immersion

An experiment was conducted by immersing the specimens in Ringer's saline (Table 2-3) for 90 days at temperature 37±1°C. The corrosion potential of the laser-molten layer and the base metal was measured three times every 30 days. Since the surface was partially laser-treated, it was not impossible to measure the corrosion resistance according to the ASTM F 2129 standard, specifically designed for implant corrosion testing [Corbett R.A., et al. 2007]. As the width of the laser-molten layers was 3-4 mm, a thin electrode was required for that purpose. Therefore, the measurements were carried out using Dentotest-Six device for measuring the corrosion potential and electromotive voltage of metal objects in the oral cavity. The first electrode was connected to the laser-molten layer, while the second was immersed in the solution at 2-4 mm distance from the specimen.

The corrosion potential measurement was carried out with the help of Assoc. Prof. Miglena Balcheva from the FDM, MU – Varna.

3.2. Electrochemical corrosion tests

Electrochemical tests were carried out at temperature 37°C in three types of corrosion media: Ringer's saline, artificial saliva (Fusayama, Meyer) and artificial saliva with high acidity (Table 2-3).

For each corrosion medium, two tests were performed:

1) Studying the change of free potential Ef until a steady value Ess was achieved;

2) Investigating the steel behavior in external anodic polarization.

Before the electrochemical corrosion test, the working surface of all specimens was polished for 15 minutes with GOI paste, washed and degreased. The degreased specimens were fixed in a Teflon holder, which opening provided a constant contact surface with the electrolyte (0.4 cm^2 for Ringer's saline and 0.28 cm^2 for artificial saliva). At a 2 mm distance from this surface, Lugin's capillary was pierced through the Teflon body, ending at the opening with a cup where the reference electrode was placed.

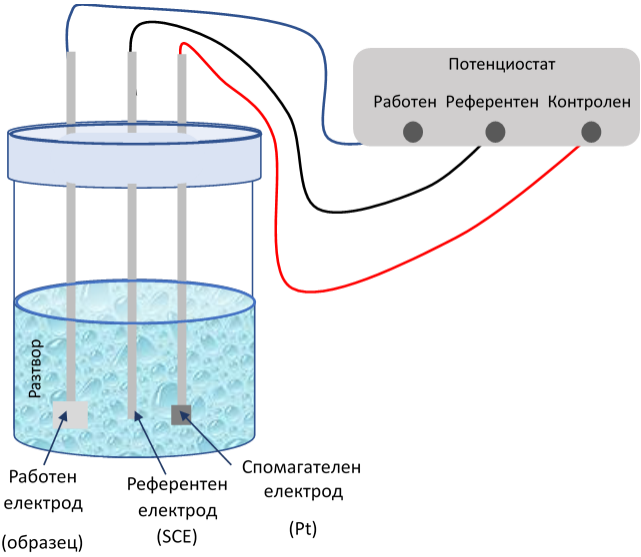

Fig. 2-2 Schematic of electrogalvanic corrosion tests according to ASTM F3044-14 standard.

The external anodic polarization was carried out using a RADELKIS OH-405 potentiostat, to which a standard three-electrode cell was connected (Fig. 2-2): the studied specimen was a working electrode; a saturated calomel electrode (SCE) was used as a reference electrode, and a platinum electrode was used as a counter electrode. The potential was changed from -550 mV to +1250 mV at a rate of 1 mV/s in tests with Ringer's saline and from -500 mV to +1000 mV at a rate of 1 mV/s in the tests with artificial saliva.

Data from both tests were collected using NI USB-6008 analog-to-digital converter, and then processed using a spreadsheet. All potential values were calculated against a normal hydrogen electrode (NHE).

The electrochemical corrosion study was carried out with the help of Assoc. Prof. Dr. Eng. Diana Tsaneva and Ch. Assistant Dr. Eng. Mariana Ilieva from RU "A. Kanchev", Ruse.

4. Specimen characterization

4.1. Surface morphology examination

Surface morphology of all specimens before and after corrosion was examined using optical microscopes Olympus SZ51 and XJL-17A equipped with digital camera No. TP6080000B.

The specimen surface and chemical composition in certain areas were examined using a scanning electron microscope (SEM) (SEM / FIB LYRA I XMU, TESCAN), equipped with EDX detector (Quantax 200, Bruker) at the Faculty of Physics, Sofia University (Fig. 2-3).

4.2. Microstructure examination

To examine the microstructure and development of cracks of laser-molten layers in depth, it was necessary to make specimens in cross-section. For this purpose, the specimens were cut along the diagonal of the area subject to corrosion tests, or as close as possible to the corrosion defects (Fig. 2-4). Cutting was carried out using BUEHLER IsoMet 15HC/IsoMet 1000 PRECISION SAW cutting machine with BUEHLER ISOCUT WAFERING BLADE HIGH CONCETRATION diamond disc (Table 2-4). Epoxy resin was poured

on the obtained specimens in special matrices and were prepared for further processing.

Each specimen was ground and polished using BUEHLER EcoMet 30 machine. Grinding was carried out in series with sandpapers of different abrasive sizes: P 400; P 800; P 1200; P 1500. After grinding with the specific sandpaper, the specimen was washed abundantly with running water and dried with hot air. Polishing was carried out in 3 stages according to the manufacturer's instructions (Table 2-4).

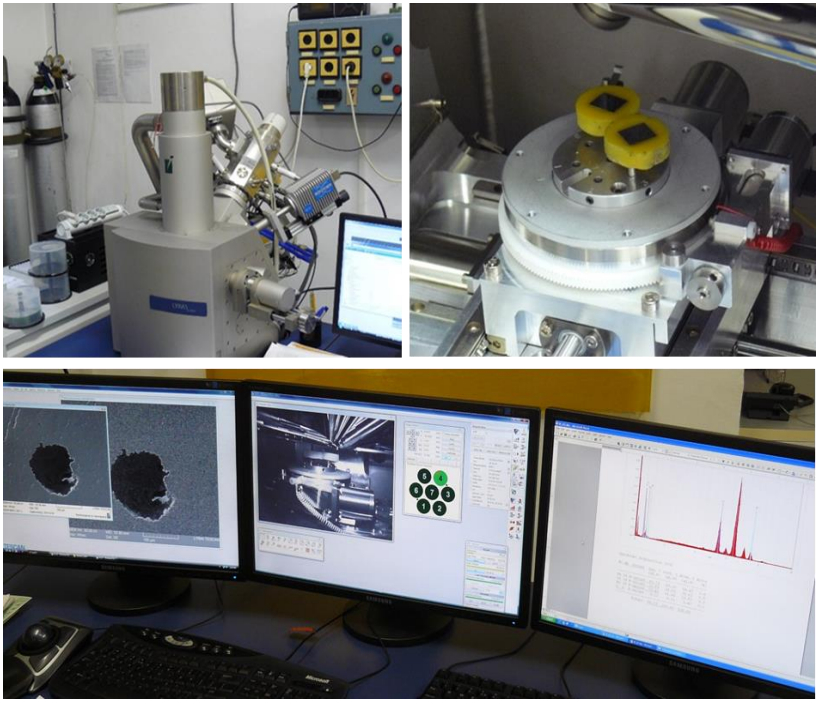

Fig. 2-3 Examination of surface morphology using SEM.

First, the specimens were polished using UltraPad disc and MetaDi Supreme diamond suspension (9 μm), then with TriDent disc and MetaDi Supreme diamond suspension (3 μm), and finally with ChemoMet disc and MasterPrep Aluminum final polishing suspension. After each polishing step, the specimens were washed successively with water and ethanol and air-dried.

The polished specimens were etched with aqua regia (3 HCl+1 HNO_3), which composition is a mixture of 3 volumetric parts of concentrated hydrochloric acid (HCl) and 1 volumetric part of concentrated nitric acid (HNO_3) [ASTM E407-99 Standard]. The manifestation of microstructure was monitored on Leica M 80 optical microscope (OM) at different magnifications (7.5, 10, 20, 40, and 60 times) and at different time intervals (30 s, 1 min, 2 min, 3 min, 4 min, and 5 min).

Table 2-4
Processes and consumables in making metallographic sections

No.	Process	Consumable	Note/Abrasive	Angular velocity, rpm	Time, min
1.	Cutting	Diamond disc	Counterweight 250 g	375	~25
2.	Grinding	Sandpaper (P400)	To flatness	300	
		Sandpaper (P800)			
		Sandpaper (P1200)			
		Sandpaper (P1500)			
3.	Polishing	Step 1 UltraPad	MetaDi Supreme 9 μm diamond suspension	150	5
		Step 2 TriDent	MetaDi Supreme 3 μm diamond suspension	150	3
		Step 3 ChemoMet	Final polishing MasterPrep Aluminum suspension	150	2

Etching of various duration was carried out to develop a methodology for the preparation of metallographic specimens in order to study the microstructure of a laser-molten layer and base metal of the same specimen. It was established that the microstructure of the laser-molten layers was visible after a shorter reagent exposure time –

2 minutes. Longer times lead to excessive corrosion and unclear structural elements. Longer time than 5 minutes was required to reveal the microstructure of the base metal. Subsequent polishing of the specimen resulted in more obscure structural features.

Based on this, an optimized procedure was proposed where the etching process should be carried out in two consecutive steps (Figs. 2-4).

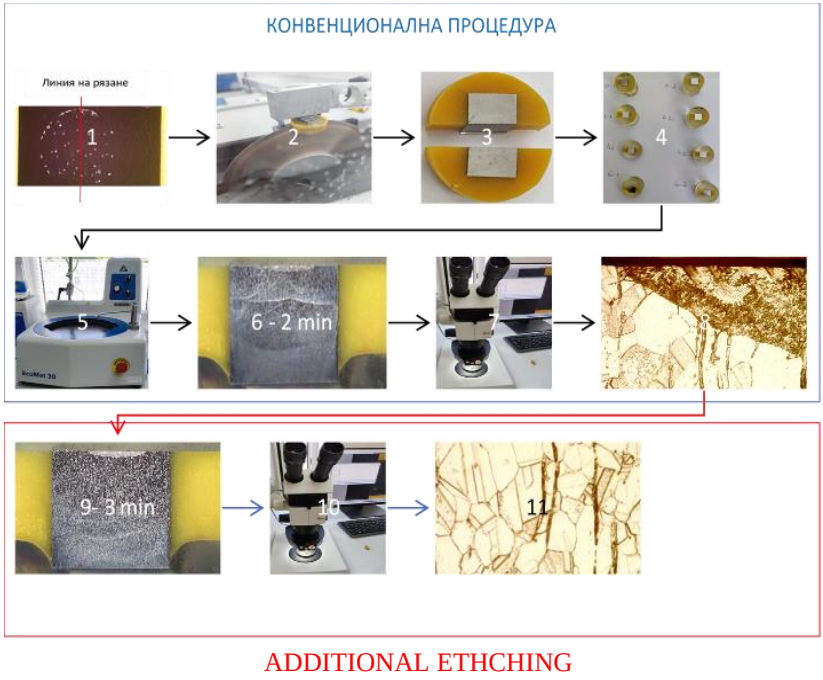

Fig. 2-4 Methodology for fabrication of metallographic specimens.

Conventional procedure: 1) inspection of the specimen; 2) cutting a specimen; 3) specimen cut; 4) specimens in epoxy resin; 5) specimen grinding and polishing; 6) visible microstructure (etching); 7) observation with an optical microscope; 8) microstructure photographs.

Additional etching: 9) additional etching to reveal the base metal microstructure, 10) OM observation, and 11) base metal microstructure.

Based on this, an optimized procedure was proposed where the etching process is carried out in two consecutive steps (Figs. 2-4).

In the first stage, the microstructure of the laser-molten layer was revealed in 2 min. After the necessary metallographic tests were carried out, it was proceeded with the second stage of the test – 3-minute additional etching to develop and examine the base metal microstructure.

The microstructure and in-depth corrosion crack development examination was carried out using OM Leica M 80 with digital camera Leica IC 90 E, OM Olympus SZ51 and OM XJL-17A with digital camera No. TP6080000B. The microstructure and chemical composition were examined using Zeiss Evo 10 SEM (Jena, Germany) equipped with Zeiss Smart EDX detector.

CHAPTER 3
AISI 321 STEEL MICROSTRUCTURE AFTER LASER SURFACE MELTING

In this chapter, AISI 321 austenitic steel surface microstructure was examined after laser melting and compared to the raw material microstructure.

It was found that before the laser treatment the microstructure was two-phase and relatively inhomogeneous in terms of morphology and chemical composition. It consisted of austenite with grain size between 20-150 μm, banded δ-ferrite and spherical carbides at the grain boundaries (Fig. 3-1 and Fig. 3-2).

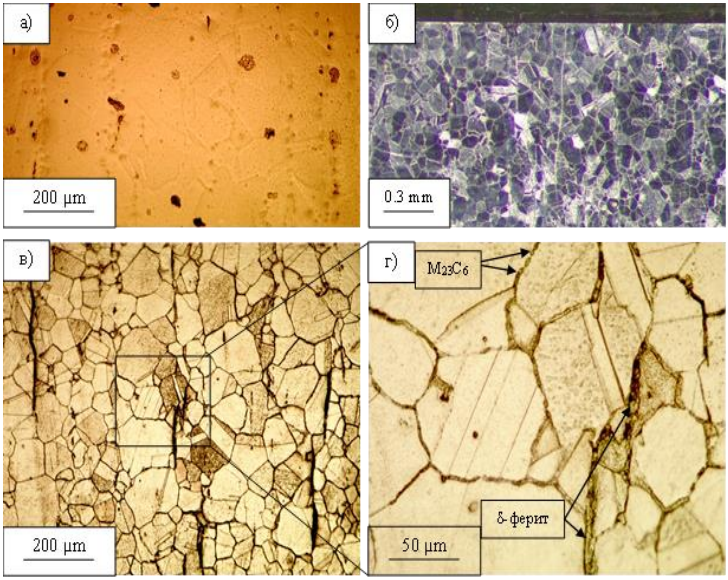

Fig. 3-1 AISI 321 austenitic steel microstructure: а) after polishing, and б), в), and г) after surface etching .

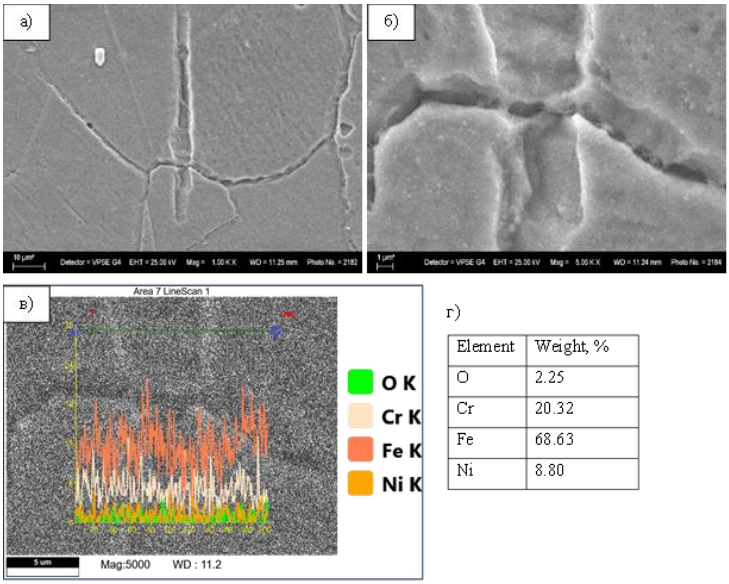

Element	Weight, %
O	2.25
Cr	20.32
Fe	68.63
Ni	8.80

Fig. 3-2 а) and б) delta-ferrite in AISI 321 austenitic steel microstructure, and в) and г) chemical composition in the δ-ferrite zone.

After laser melting, the two-phase microstructure (δ-ferrite and austenite) was preserved; however, it become more homogeneous in terms of morphology and composition (Fig. 3-3, Fig. 3-4, Fig. 3-5, and Fig. 3-6).

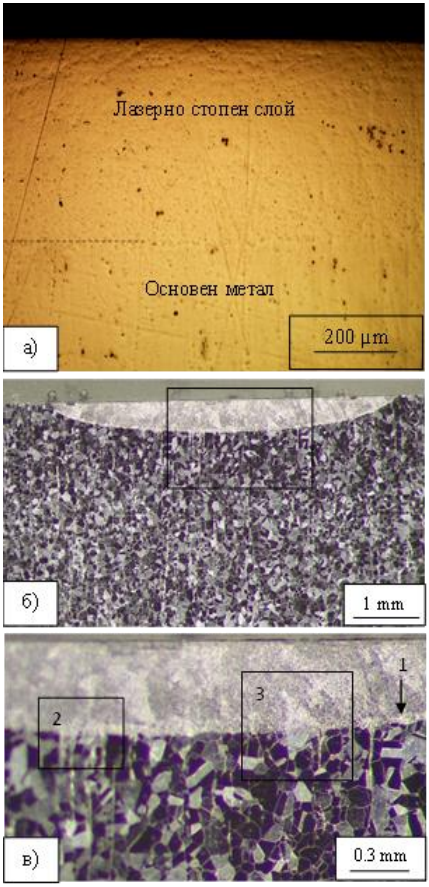

Fig. 3-3 AISI 321 austenitic steel laser-molten surface layer microstructure: а) after polishing, and б) and в) after surface etching (Specimen 4).

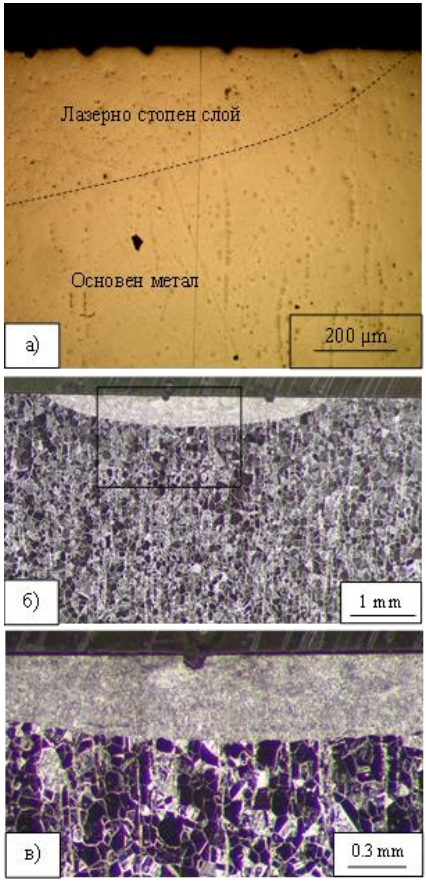

Fig. 3-4 AISI 321 austenitic steel laser-molten surface layer microstructure: а) after polishing, and б) and в) after surface etching (Specimen 6).

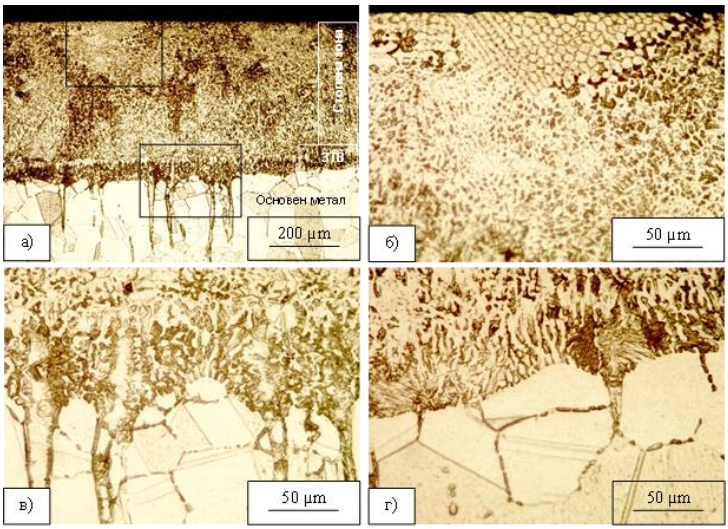

Fig. 3-5 а) AISI 321 austenitic steel molten surface layer microstructure, б) on the surface, в) and г) and in the boundary layer with the base metal.

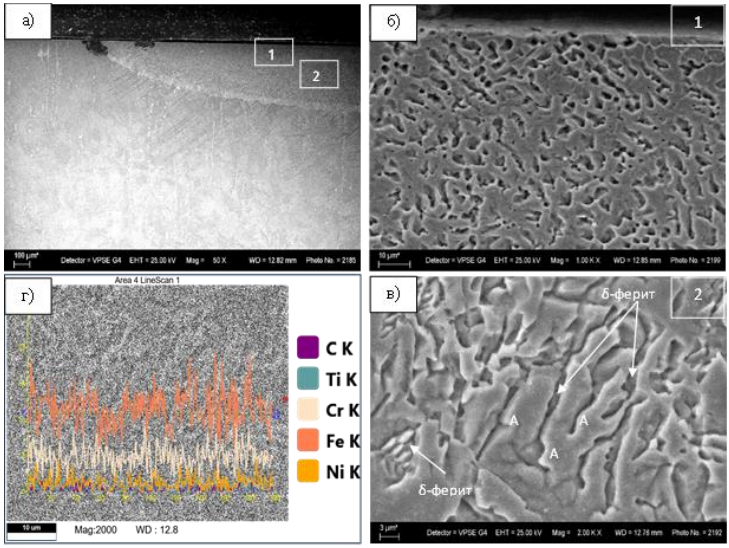

Fig. 3-6 а), б), в) AISI 321 austenitic steel molten surface layer microstructure, and г) chemical composition in the molten zone (A – austenite).

The different dendrite morphology in the various zones of the molten layer was confirmed: fine equiaxed dendrites on the surface and columnar dendrites at the bottom of the molten bath (Fig. 3-5 and Fig. 3-6). Delta-ferrite was localized in the interdendritic spaces and was in larger quantities in the transition zone between the molten layer and the base metal (Fig. 3-6).

CHAPTER 4
CORROSION OF LASER-MOLTEN AISI 321 STEEL LAYERS IN RINGER'S SALINE

In this chapter, the corrosion behavior of AISI 321 austenitic steel base metal and laser-molten layers in Ringer's saline, was examined. Two types of experiments were conducted: by immersing the specimens in the corrosion medium for a 3-month period and electrochemical corrosion.

After 3-month specimen immersion testing, it was found that the melting laser surface treatment did not lead to any significant changes in the corrosion behavior of AISI 321 austenitic steel.

The average corrosion potential of the molten layers (+163 mV to +223 mV) was higher than that of the base metal, but within reference values (Fig. 4-3). No corrosion changes were observed in the surface or in-depth microstructure of either the base metal or the molten layers.

During the electrochemical corrosion experiment, the free potential Ef of the base metal (+94 mV) was decreased, while the Ef of the laser-molten layers was shifted to more positive values (+233 mV) (Fig. 4-4). The pitting potentials Epit of all laser-molten layers were practically equal (+505 mV/+536 mV) and were higher than the Epit of the base metal (+348 mV) (Fig. 4-5).

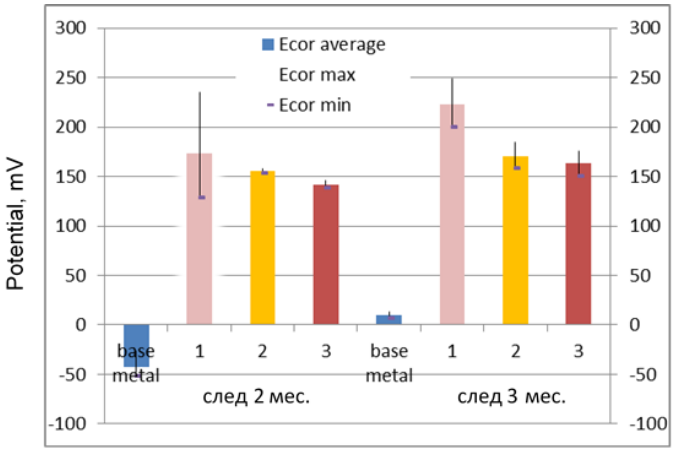

Fig. 4-3 AISI 321 steel and laser-molten layers' corrosion potential after being immersed in Ringer's saline for 2 and 3 months: 1) specimen 1 Ev=31.7x10^3 J/cm^3 (specimen 1); 2) specimen 4 Ev=34x10^3 J/cm^3 (specimen 4), and 3) specimen 6 Ev=28.3x10^3 J/cm^3 (specimen 6).

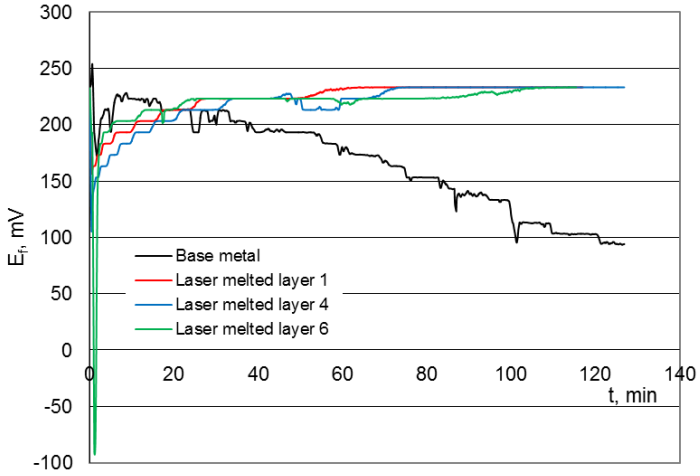

Fig. 4-4 Free potentials Ef of the base metal and laser-molten layers of specimen 1 (Ev=31.7x10^3 J/cm^3), specimen 4 (Ev=34x10^3 J/cm^3) and specimen 6 (Ev=28.3x10^3 J/cm^3)

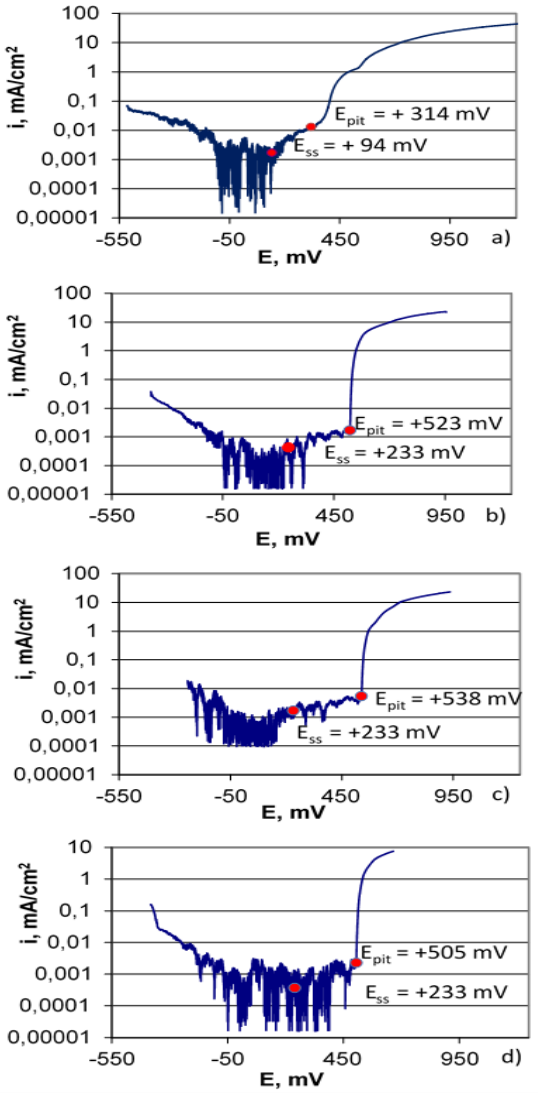

Fig. 4-5 a) Potentiodynamic curves of the base metal, b) laser-molten layer of specimen 1 (Ev=31.7x10^3 J/cm^3), c) specimen 4 (Ev=34x10^3 J/cm^3), and d) speciment 6 (Ev =28.3x10^3 J/cm^3)

After electrochemical corrosion tests, pitting and crevice corrosion was observed on the surface of all specimens, either untreated or laser-molten (Fig. 4-7 and Fig. 4-9).

Corrosion pitting on the surface of the base metal was characterized by an irregular shape and sizes between 20-100 μm (Fig. 4-7). While pitting on the laser-molten surfaces had a random distribution, with

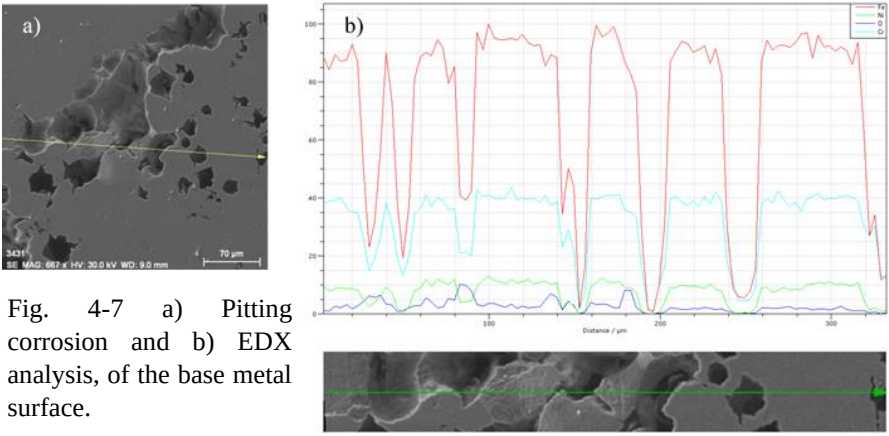

Fig. 4-7 a) Pitting corrosion and b) EDX analysis, of the base metal surface.

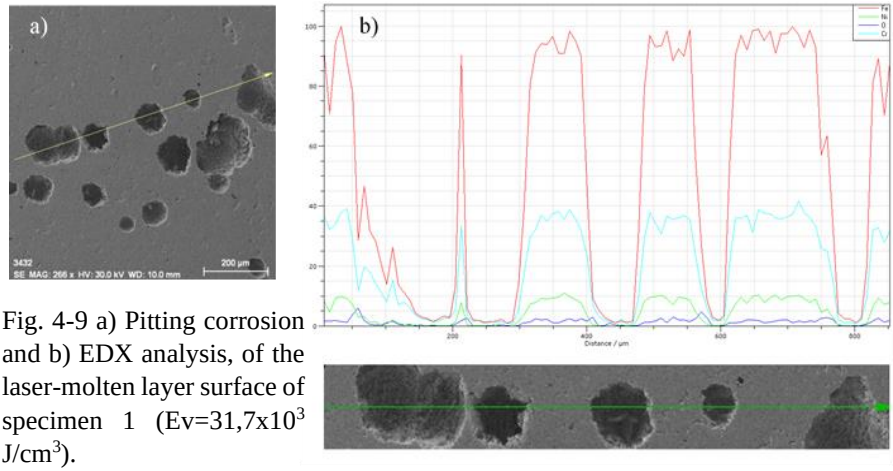

Fig. 4-9 a) Pitting corrosion and b) EDX analysis, of the laser-molten layer surface of specimen 1 (Ev=31,7x10^3 J/cm^3).

regular equiaxed shape and larger sizes between 50-250 μm (Fig. 4-9).

Laser-molten layers were characterized by an improved structure of the passive layer after the electrochemical tests in Ringer's saline due to the refined and involvement-free surface microstructure.

The electrochemical examination showed increased resistance to pitting corrosion of AISI 321 austenitic stainless-steel laser-molten layers, which was due to the more homogeneous and fine-grained microstructure and the improved passive layer on the surface.

CHAPTER 5
DESTRUCTION OF LASER-MOLTEN AISI 321 STEEL LAYERS IN RINGER'S SALINE

In this chapter, the destruction of AISI 321 austenitic steel base metal and laser-molten layers after electrochemical corrosion tests in Ringer's saline, was examined. An analysis of the surface morphology and development of in-depth corrosion pitting of the metal was carried out.

A presence of corrosion pitting of various shapes and sizes was found on the surface of all specimens (Fig. 5-2).

The pittings on the raw steel surface was irregularly shaped, smooth-walled, of size between 10-300 μm.

The pittings on the surface of the laser-molten layers had rounded shape, sizes of 10-400 μm, less depth and rough walls.

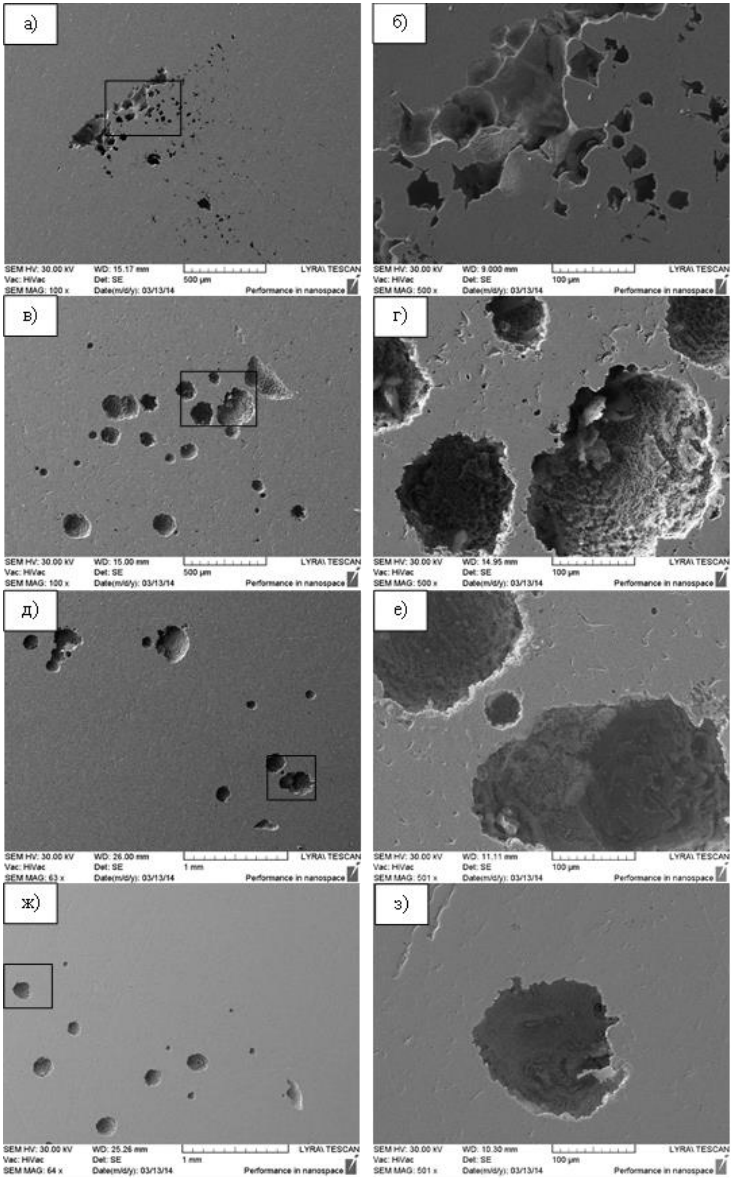

Fig. 5-2 а), б) Corrosion damage on the surface of AISI 321 austenitic steel: specimen 0, в) and г) after laser melting of the surface layer: specimen 1, д) and е) specimen 4, and ж) and з) specimen 6 (SEM investigation).

The corrosion destruction of AISI 321 austenitic stainless steel surface layer was selective, mainly of δ-ferrite, in the form of pittings of irregular shape and great depth (50-300 μm (Fig. 5-4 and Fig. 5-5)). Intergranular corrosion was present at the austenite grain boundaries near the surface (Fig. 5-4).

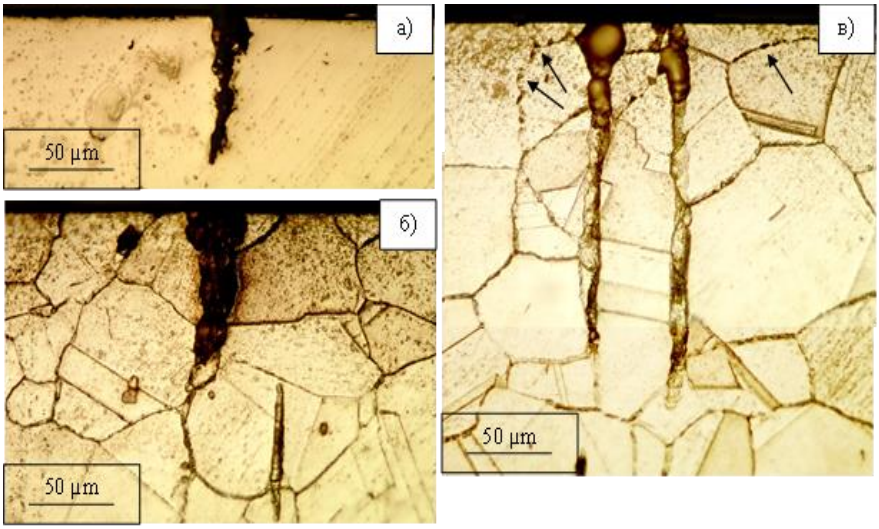

Fig. 5-4 Development of corrosion cracks in depth in AISI 321 austenitic steel (specimen 0). The intergranular corrosion is indicated by arrows.

The corrosion destruction of laser-molten AISI 321 steel layers was selective by δ-ferrite destruction in the form of shallow (40-100 μm) equiaxed pitting (Fig. 5-8 and Fig. 5-10).

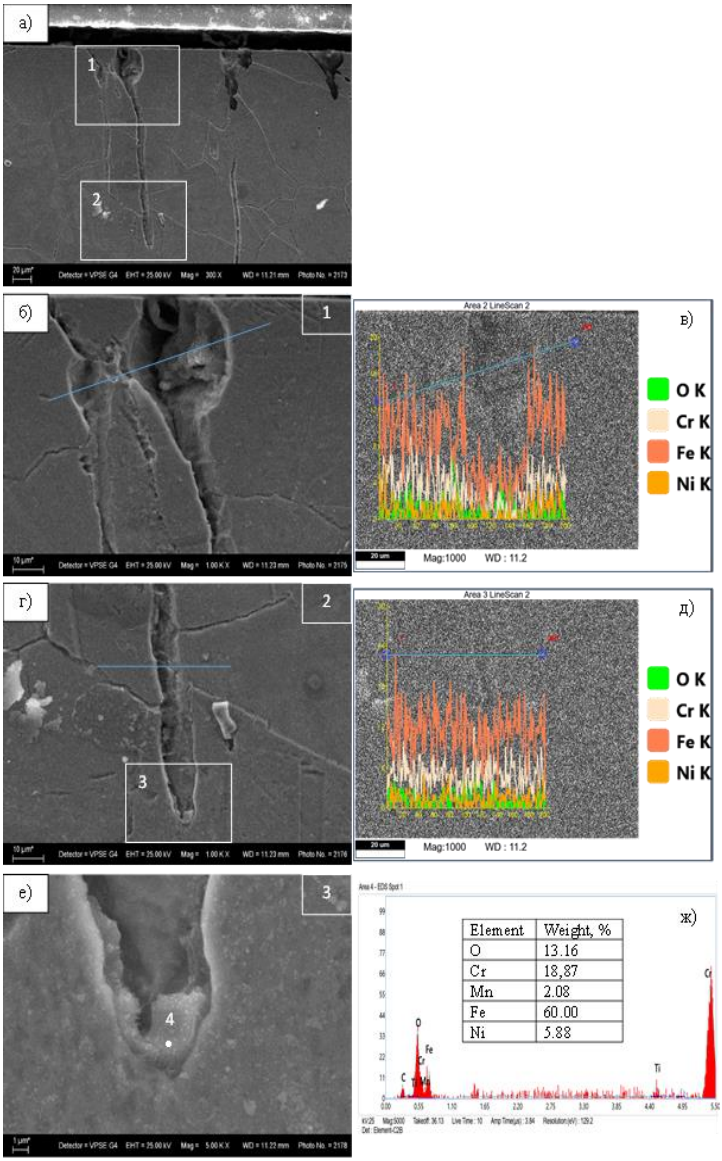

Fig. 5-5 Chemical composition in AISI 321 austenitic steel corrosion crack (specimen 0).

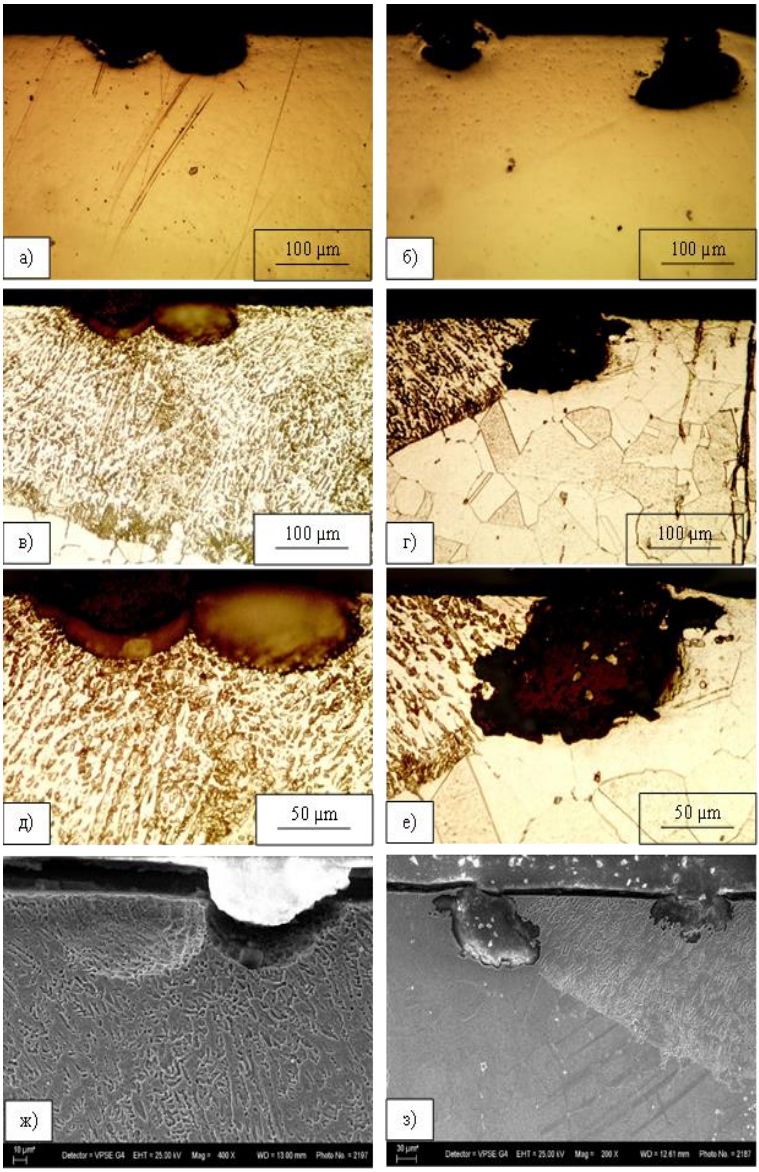

Fig. 5-8 Development of in-depth corrosion distruction of a laser-molten austenitic AISI 321 steel layer (specimen 4): а), б) after polishing, в) to з) and after the microstructure is revealed (OM images from а) to е) and SEM images – ж) and з)).

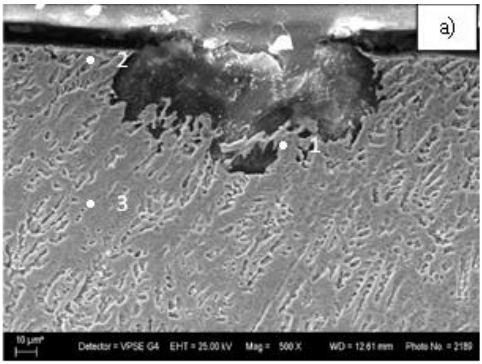

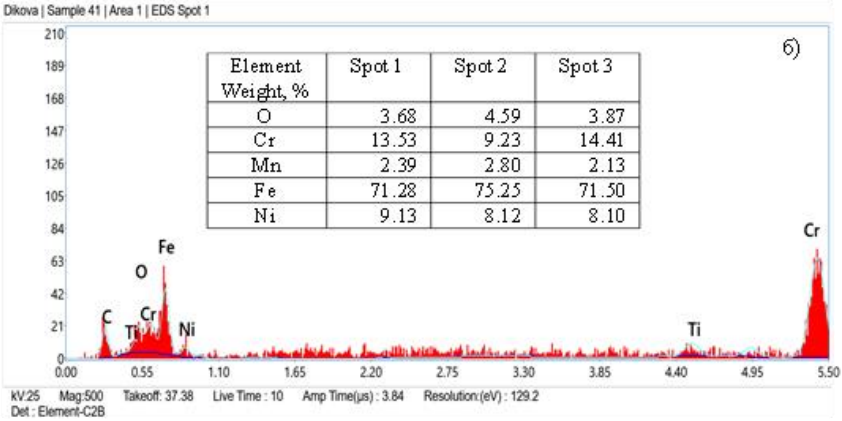

Element Weight, %	Spot 1	Spot 2	Spot 3
O	3.68	4.59	3.87
Cr	13.53	9.23	14.41
Mn	2.39	2.80	2.13
Fe	71.28	75.25	71.50
Ni	9.13	8.12	8.10

Fig. 5-10 а) in-depth corrosion distruction of a laser-molten austenitic AISI 321 steel layer, and б) chemical composition at various points (specimen 4).

It was found out that the main mechanism of corrosion destruction in AISI 321 austenitic stainless steel with no surface treatment and after laser melting was identical – selective destruction of the corrosion-resistant δ-ferrite phase in the form of pitting. However, the morphology and size of corrosion pitting was different, which was determined by the δ-ferrite morphology in the microstructure.

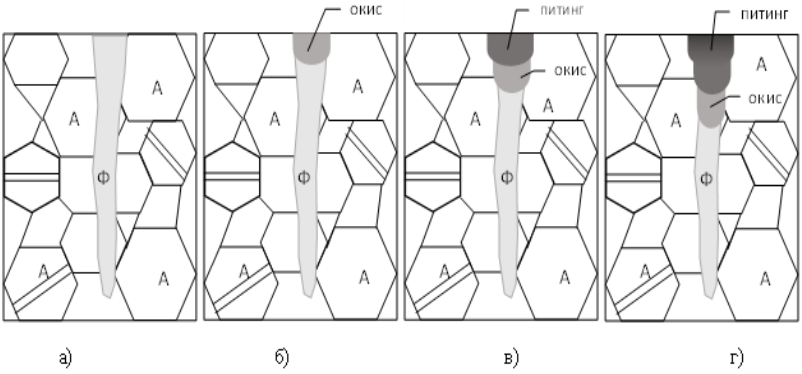

Fig. 5-12 Mechanism of selective corrosion destruction of AISI 321 austenitic steel by δ-ferrite oxidation on Fig. 5-4в (A – austenite, F – ferrite).

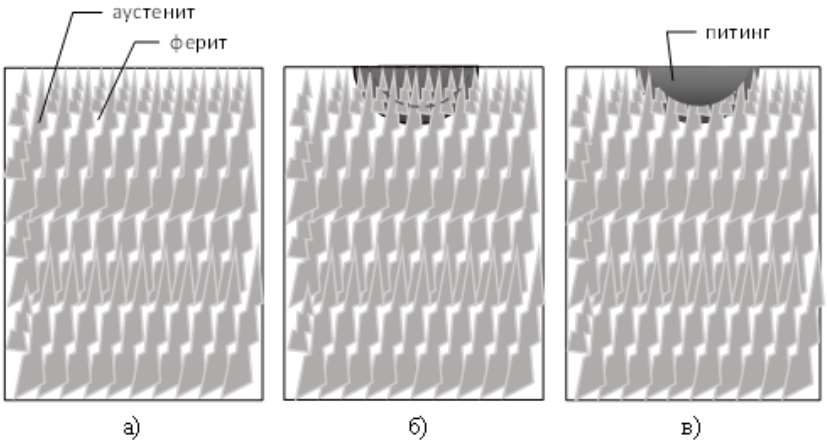

Fig. 5-13 Mechanism of selective corrosion of a laser-molten AISI 321 steel layer on Fig. 5-10a: а) schematically presented microstructure, б) destruction of δ-ferrite and network of austenite dendrites, and в) pitting formed after the austenite dendrite destruction.

Consequently, from the point of view of corrosion resistance, laser melting of AISI 321 steel surface created more favorable conditions for the durability of the implant structure.

CHAPTER 6
ELECTRO-CHEMICAL CORROSION OF LASER-MOLTEN AUSTENITE AISI 321 STEEL LAYERS IN ARTIFICIAL SALIVA

Dental materials in the oral cavity interact continuously with physiological fluids. These are subject to both chemical and physical impacts, as well as to the metabolism of approximately 30 types of bacteria [Chaturvedi T.P., 2008]. Saliva is a hypotonic solution containing bioactonate, chloride, potassium, sodium, nitrogen compounds and proteins [Martinez J.R. and Barker S., 1987]. Salivary acidity (pH) ranges between 5.2 and 7.8. Corrosion, i.e., the gradual degradation of materials under electrochemical impact is of great importance, especially when orthodontic appliances and other metal structures are placed in the electrolyte environment of the human mouth [Maijer R. and Smith D.C., 1982; Maijer R. and Smith D.C., 1986]. Temperature, quantity and quality of saliva, plaque, pH, proteins, food properties and oral conditions are the main factors that influence corrosion processes.

In this chapter, the electrochemical corrosion of laser-molten AISI 321 austenitic stainless steel layers after the tests in artificial saliva (AS) of different acidity, i.e., pH 5.6 and pH 6.5, was investigated.

In the electrochemical corrosion test in artificial saliva with higher acidity (pH 5.6), all tested specimens showed the presence of pinhole corrosion (Fig. 6-1 and Fig. 6-2).

Regardless of the medium acidity, two types of corrosion were observed on the surface of all specimens: pitting and crevice. The pittings formed were relatively small in size, 150-300 μm, and their number is larger in the laser-treated specimens compared to those of the base metal.

The deteriorated corrosion behavior of the laser-molten surfaces was expressed in decreased stationary and pitting potentials of all treated specimens compared to the base metal (Fig. 6-5, Fig. 6-8, and Table 6-2).

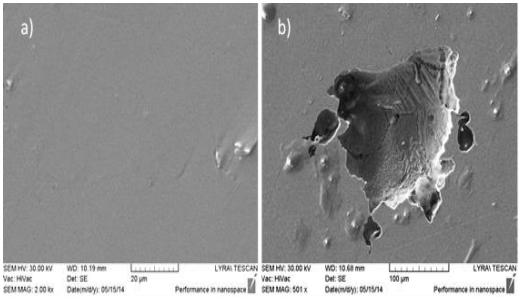

Fig. 6-1 a) Base metal surface morphology before and б) after the electrochemical corrosion test (pitting corrosion).

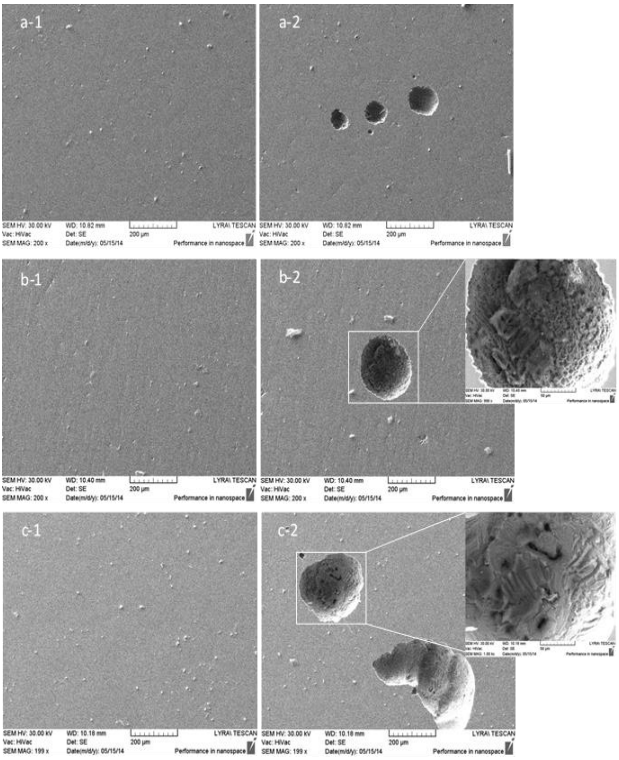

Fig. 6-2 a) Laser-molten surface layer morphology of specimen 1 (Ev=31.7x10^3 J/cm^3), b) specimen 4 (Ev=34x10^3 J/cm3), and c) specimen 6 (Ev=28.3x10^3 J/cm^3) before (a-1, b-1, and c-1) and after (a-2, b-2, and c-2) electrochemical corrosion).

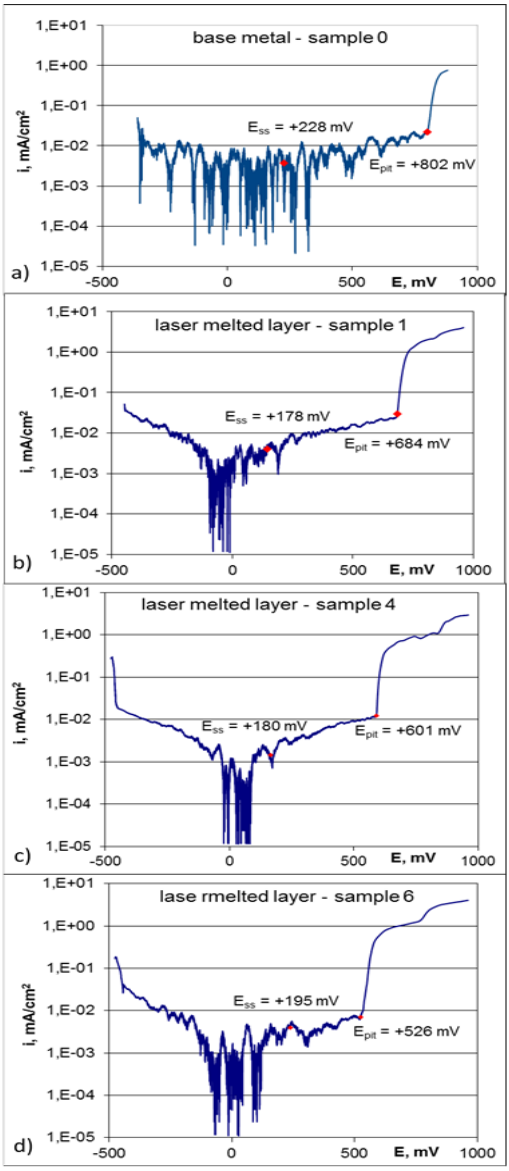

Fig. 6-5 a) Potentiodynamic curves of the base metal, b) laser-molten layers, of specimen 1 (Ev=31.7x10^3 J/cm^3), c) specimen 4 (Ev=34x10^3 J/cm^3), and specimen 6 (Ev =28.3x10^3 J/cm^3.

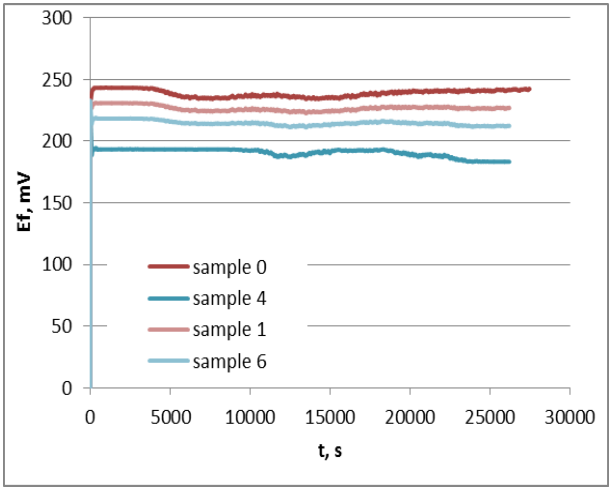

Fig. 6-8 Change of the free potentials Ef over time during the electrochemical corrosion in artificial saliva at pH 5.6.

Table 6-2
Stationary Ess and pitting Epit potential values of base metal (specimen 0) and laser-molten layers (specimens 1, 4 and 6) in electrochemical corrosion tests.

Specimen	pH 6,5		pH 5,6	
	E_{ss}, *mV*	E_{pit}, *mV*	E_{ss}, *mV*	E_{pit}, *mV*
0	+215	+534	+238	+802
1	+223	+605	+178	+684
4	+233	+530	+180	+601
6	+213	+730	+195	+526

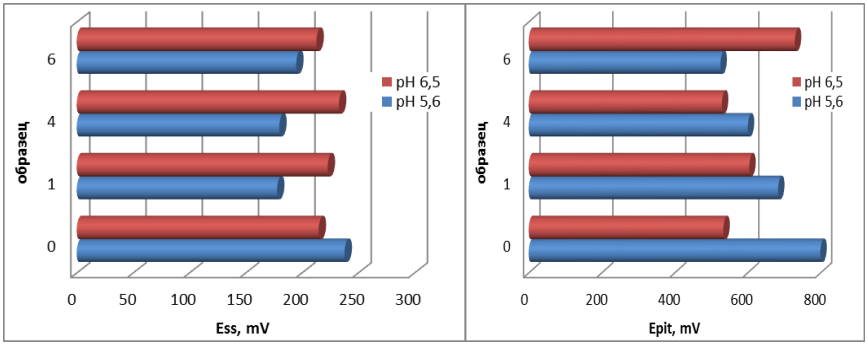

а) б)

Fig. 6-9 a) Stationary Ess potentials, b) pitting Epit potentials of base metal (specimen 0) and laser-melted layers (specimens 1, 4 and 6) during electrochemical corrosion tests in artificial saliva of different acidity.

Comparative electrochemical tests of AISI 321 steel base metal and laser-molten layers demonstrate different resistance to corrosion in artificial saliva of various acidity – pH 6.5 and pH 5.6 (Fig. 6-9 and Table 6-2).

During the tests in pH 6.5 artificial saliva, no sharp boundary for the Ess and Epit values of the base metal and laser-molted layers was noted. The pitting potentials Epit of the laser-molten layers were slightly higher than those of the base metal by 70-200 mV (Fig. 6-9 and Table 6-2).

However, in electrochemical corrosion in pH 5.6 artificial saliva, the laser-molten surface layers showed lower resistance to pitting corrosion than the base metal. Pitting occurred at smaller pitting potentials Epit (+526/+684 mV), while for the base metal Epit was +802 mV (Fig. 6-9 and Table 6-2).

The reduced corrosion resistance of austenitic stainless steel laser-molten layers in pH 5.6 artificial saliva is mainly due to the medium acidity.

GENERAL CONCLUSIONS

1. It was confirmed that AISI 321 austenitic stainless steel microstructure is two-phase, relatively inhomogeneous in terms of morphology and chemical composition. It consists of austenite with a grain size between 20-150 μm, banded δ-ferrite and spherical carbides along the grain boundaries.
2. The microstructure of the laser-molten layer was also confirmed to be two-phase (δ-ferrite and austenite), however more homogeneous in terms of morphology and composition. The different morphology of dendrites in the individual zones of the molten layer was confirmed: fine equiaxed on the surface and columnar at the bottom of the molten pool. Delta-ferrite is located in the interdendritic spaces and is in larger quantities in the transition zone between the molten layer and the base metal.
3. It was found that laser surface treatment by melting did not lead to any significant changes in AISI 321 austenitic steel corrosion behavior after 3-month corrosion tests by immersing the specimens in Ringer's saline.
4. Electrochemical corrosion tests in Ringer's saline showed that AISI 321 austenitic stainless steel laser-molten layers (pitting potentials Epit +505 mV/+536 mV) demonstrated increased resistance to pitting corrosion compared to untreated steel (Epit +348mV), which was due to both the more homogeneous and fine-grained microstructure and the improved passive layer on the surface.
5. It was found that the main mechanism of corrosion damage in Ringer's saline in AISI 321 austenitic stainless steel with no surface treatment and after laser melting is identical: selective destruction of the corrosion-resistant δ-ferrite phase in the form of pitting. However, the morphology and size of corrosion pitting was different, which was determined by the δ-ferrite morphology in the microstructure.
6. It was found that the pitting on the untreated steel surface had irregular shape, smooth walls of size between 10-300 μm and depth 50-300 μm. Intergranular corrosion was present at the austenite grain boundaries near the surface.

7. The pittings on the surface of the laser-melted layers were found to have rounded shape, sizes 10-400 μm, more shallow depth (40-100 μm) and uneven walls.

8. During the electrochemical tests, it was found that AISI 321 steel base metal and laser-molten layers showed different resistance to corrosion in artificial saliva of various acidity, i.e., pH 6.5 and pH 5.6.

9. It was found that there was no significant difference in pitting potentials of the base metal and laser-molten layers (Epit of the molten layers are higher than those of the base metal by 70-200 mV) in pH 6.5 artificial saliva, which was a sign of similar corrosion resistance.

10. In pH 5.6 artificial saliva, laser-molten surface layers (Epit +526/+684 mV) were found to show lower resistance to pitting corrosion than the base metal (Epit +802 mV), which was mainly due on the medium acidity.

11. It was confirmed that two types of corrosion were present on the surface of all specimens: pitting and crevice, regardless of the medium (artificial saliva) acidity. The pittings formed were 150-300 μm in size, and their number was higher in the laser treated samples compared to those of the base metal.

12. In terms of corrosion resistance, AISI 321 steel surface laser melting created more favorable conditions for the durability of the implant dtructure in Ringer's saline and pH 6.5 artificial saliva.

CONTRIBUTIONS

1. Scientific and applied contributions

1.1. Original

1.1.1. It was found that the laser surface treatment by melting did not lead to any significant changes in AISI 321 austenitic steel corrosion behavior after the corrosion tests by immersing the specimens in Ringer saline.

1.1.2. It was found that laser-molten AISI 321 steel layers (pitting potentials Epit +505 mV/+ 536 mV) showed increased resistance to pitting corrosion in Ringer saline compared to untreated steel (Epit +348 mV).

1.1.3. It was found that the main mechanism of corrosion destruction of AISI 321 austenitic stainless steel with no surface treatment and after laser melting is identical: selective destruction of the corrosion-unstable δ-ferrite phase in the form of pitting.

1.1.4. The morphology and sizes of corrosion pitting were found to be different, which was determined by the δ-ferrite morphology in the microstructure. The pittings on the surface of the laser-molten layers had a rounded shape and smaller depth (40-100 μm) compared to those on the untreated surface.

1.1.5. AISI 321 steel base metal and laser-molten layers were found to show different corrosion resistance in artificial saliva of various acidity. Corrosion resistance of the base metal and laser-molten layers in pH 6.5 artificial saliva was similar, however at increased acidity (pH 5.6), the laser-molten layers showed lower pitting corrosion resistance.

1.2. Confirmatory

1.2.1. It was confirmed that the AISI 321 austenitic stainless steel microstructure was two-phase and consisted of austenite, banded δ-ferrite and spherical carbides on the grain boundaries.

1.2.2. It was confirmed that the laser-molted layer microstructure is two-phase (δ-ferrite and austenite) with dendritic morphology and relatively homogeneous composition.

1.2.3. It was confirmed that two types of corrosion were observed on the surface of untreated and laser-molden AISI 321 austenitic stainless steel – pitting and crevice, regardless of the medium type and acidity.

1.2.4. It was confirmed that intergranular corrosion was present at the austenite grain boundaries near the surface of untreated AISI 321 steel.

2. Applied contributions

2.1. Original

2.1.1. An optimized methodology for preparation of austenitic stainless steel microsands was proposed for the examination the microstructure of the base metal and laser-molten layer of the same specimen.

2.1.2. Laser technologies leading to melting of surface layers can be used to fabricate implants and other structures from austenitic stainless steel to be used in biological fluids with composition and acidity close to those of Ringer's saline and pH 6.5 artificial saliva.

2.1.3. It is not recommended to use laser technologies with austenitic steel melting for the fabrication of implants and other structures to be used in increased acidity media.

CONCLUSION

In this dissertation, the corrosion resistance of AISI 321 austenitic stainless steel in biological fluids after laser surface treatment, was investigated. Initially, the steel surface microstructure after laser melting was investigated and compared with untreated material microstructure. Then, the corrosion resistance and corrosion destruction mechanism of AISI 321 steel laser-molten layers in Ringer's saline, were examined. A comparative analysis of the electrochemical corrosion in artificial saliva with various acidity was also made.

It was found that:

1) In Ringer's solution, AISI 321 steel laser-melted layers show increased corrosion resistance compared to untreated steel;

2) In pH 6.5 artificial saliva, the corrosion resistance of the laser-melted layers and the base metal is similar;

3) In artificial saliva with increased acidity pH 5.6, the laser-molten layers have lower corrosion resistance.

Based on the obtained results, recommendations have been made on the use of laser technologies in implants, dental structures and medical device fablication from AISI 321 austenitic stainless steel.

DISSERTATION RELATED PUBLICATIONS

1. Ivaylo Parushev, Natalina Panova, Krastena Nikolova, Tsanka Dikova; Corrosion in biological fluids of chrome-nickel stainless steel after laser; VII International Scientific Conference Summer Session "INDUSTRY 4.0"; 22-25.06.2022, Varna, Bulgaria; session: Dominant Technologies in "INDUSTRY 4.0", volume 1/14; p.38-44;
2. Natalina K. Panova, Krastena T. Nikolova, Tsanka D. Dikova; Application of lasers and laser processing technologies in modern dentistry: A review; Journal of Chemical Technology and Metallurgy, 58, 6, 2023, p. 1116-1127, Q3; SCOPUS-SJR for 2021: 0.253; Impact Score: 0.81;
3. Tsanka Dikova, Natalina Panova, Ivaylo Parushev; Optimization of metallographic methodology for the study of laser-melted layers of austenitic stainless steel; Scripta Scientifica Medicine Dentalis, 2023; 9(2):35-41; DOI: 10.14748/ssmd.v9i2.9285;
4. Tsanka D. Dikova, Natalina K. Panova, Ivaylo D. Parushev; Investigation microstructure of AISI 321 stainless steel after laser surface melting; Journal of Chemical Technology and Metallurgy, 59, 1, 2024, p. 207-214, DOI: 10.59957/jctm.v59.i1.2024.24; Q3; SCOPUS-SJR for 2021: 0.253; Impact Score: 0.81.

PARTICIPATION IN SCIENTIFIC FORUMS

1. Ivaylo Parushev, Natalina Panova, Krastena Nikolova, Tsanka Dikova; Corrosion in biological fluids of chrome-nickel stainless steel after laser; VII International Scientific Conference Summer Session "INDUSTRY 4.0"; 22-25.06.2022, Varna, Bulgaria; session: Dominant Technologies in "INDUSTRY 4.0".

PARTICIPATION IN SCIENTIFIC PROJECTS

1. Project №. 21003 financed under the "Science" Fund

"Corrosion in biological fluids of chrome-nickel stainless steel after laser exposure"; Supervisor: Prof. Tsanka Dimitrova Dikova, Dr Tech; Administrative and Financial Officer: Natalina Konstantinova Panova.